Surface Structural Analysis of LiF(100) Thin Films Grown on Pt(111)

J. G. Roberts[a,b], M. A. Van Hove[b,c,d,*] and G. A. Somorjai[a,b]

[a]Department of Chemistry, University of California, Berkeley, CA 94720, USA

[b]Materials Sciences Division, Lawrence Berkeley National Laboratory, University of California, Berkeley, CA 94720, USA

[c]Advanced Light Source, Lawrence Berkeley National Laboratory, University of California, Berkeley, CA 94720, USA

[c]Physics Department, University of California, Davis CA 95616, USA

*Corresponding author. Fax: (+1) 510 4865530; e-mail: vanhove@lbl.gov

to be submitted to Surface Science

ABSTRACT

The surface structure of a multilayer LiF(100) thin film grown on Pt(111) from the vapor has been determined by the automated tensor low energy electron diffraction (LEED) method. The final structure, which refined to a Pendry R-factor (R_P) of 0.24, had a surface corrugation (Δ_1) of 0.24±0.04 Å due to the Li^+ being displaced towards the bulk, leaving the initially coplanar F^- unshifted. A similar intralayer corrugation due to the movement of the Li^+ was also observed in the layer immediately under the surface layer, although to a lesser degree: Δ_2=0.07±0.04 Å. This asymmetric relaxation resulted in the reduction of the first interlayer spacing, $d(F_2\text{-}Li_1)$, to 1.77±0.06 Å from the ideal value of 2.01Å. The second interlayer spacing, $d(Li_3\text{-}F_2)$, was within error bars of the bulk value, 2.01Å.

1. INTRODUCTION

Previous surface structural investigations of LiF have focused on the bulk cleaved LiF(100) surface that can easily be produced in vacuum and was expected to be essentially unchanged from its bulk structure [1-4]. The ideally terminated surface has a square checkerboard lattice of coplanar alternating Li^+ cations and F^- anions. Early results indicated, however, that the surface structure of this "ideal" ionic compound may be markedly different from its bulk structure. One of the first quantitative low energy electron diffraction (LEED) intensity analyses was performed on LiF(100) cleaved in vacuo; it used a nonrelativistic model for the scattering properties and did not benefit from a R-factor directed structure search [1]. After visual inspection of the correspondence between the theoretical and experimental diffraction intensity versus electron energy (I-V) curves, the surface was deemed to possess a 0.25 Å surface corrugation as a result of the Li^+ ions being displaced towards the bulk. Due to the simplicity of the model used, the reliability of this finding was in question, especially when additional structural studies did not confirm this structure. In fact, He atom scattering experiments have concluded the contrary; a surface structure with the Li^+ displaced towards vacuum by 0.307±0.003 Å from its bulk position [2]. To confuse the issue further, another structural method, low energy positron diffraction, reported that the ions maintain their bulk positions to within 0.01 Å [3].

Minor differences are expected in the final structures determined by these varying methods, since the interactions between the interrogating particles and the LiF surface are quite different. However, the difference in surface structure determined using the various techniques are not minor. With the power of a fully dynamical LEED theory aided by an R-factor directed automated search, the surface structure determination of LiF(100) was revisited in the present work. The final structure, which refined to a Pendry R-factor (R_P) of 0.24 (see Table 1), has a surface corrugation of 0.24±0.04 Å due to the surface Li^+ being displaced towards the bulk. A similar displacement of the Li^+ was also observed in the layer immediately under the surface layer, although to a lesser degree, 0.07±0.04 Å. The surface anions remain at their bulk positions. This asymmetric relaxation resulted in the reduction of the first interlayer spacing to 1.77±0.06 Å from the ideal value of 2.01 Å. The second interlayer spacing was within error bars of the bulk value.

All LEED data were obtained by ordering a multilayer film of LiF onto a conductive substrate, a deviation from the historic bulk cleaving experiments. This method has been applied successfully in the surface structural investigations of other large band gap materials [5-8]. More specifically, it was used in the surface structure determination of NaCl(100), whose LEED determined structure is analogous to the LiF(100) surface structure [7], see Table 2. A key similarity is the corrugation of the NaCl(100) surface due to the cation being 0.12 Å below the surface anions. Also, the anions remain essentially at their bulk-like positions,

resulting in the compression of the first interlayer spacing (the distance between the surface layer and the layer immediately below it) by 3.5%. Although the structure is qualitatively similar, the values of the corrugation differ greatly. The magnitude of surface corrugation is 0.12 Å for NaCl(100) and 0.24 Å for LiF(100). The other difference was the remaining intralayer corrugation in the second layer in LiF(100), a feature which is absent in NaCl(100).

2. EXPERIMENTAL METHODS AND OBSERVATIONS

2.1 Sample preparation

All experiments were performed in a stainless steel ultra high vacuum (UHV) chamber, with a base pressure of $<5x10^{-10}$ Torr, equipped with a PHI model 15-155 cylindrical mirror analyzer with an on-axis electron gun for Auger electron spectroscopy (AES) and a UTI 100C quadrupole mass analyzer for temperature programmed desorption (TPD). The Pt(111) oriented crystal was prepared from a commercially available boule with standard metallurgical methods. The crystal was spot welded to an off-axis manipulator with capabilities for electron bombardment heating to 1300 K from a rear mounted W filament and cooling to 110 K from an attached liquid nitrogen reservoir. The temperature was monitored with a chromel-alumel thermocouple spot welded to the substrate's back face. The major contaminant, as measured by AES, was carbon, and it was removed by repeated oxidative annealings at a surface temperature of 1100 K in

$5x10^{-8}$ Torr of O_2. Subsequent crystal annealing (2-3 hours) in vacuum provided a sharp LEED pattern.

2.2. Growth, Ordering and Desorption of LiF Films on Pt(111)

A similar method to that employed in the growth of NaCl thin films was utilized in the growth and ordering of LiF on Pt(111) [8]. LiF was successfully ordered by exposing the substrate, held at an elevated temperature (523 K) , to the LiF vapor emitted from a Knudsen cell operating at 890 K for 15 minutes. Additional annealing to higher temperatures,565 K, was then performed to induce further ordering of the film.

The first step in finding the optimum substrate temperature for deposition was to collect temperature programmed desorption (TPD) spectra for the LiF/Pt(111) systems. Figure 1 shows the desorption profile of the Li_2F peak, m/e=33, adsorbed on Pt(111). The lone feature exhibits an exponentially rising initial rate with a sharp falling edge. Such a profile is indicative of multilayer desorption [9,10]. Additional TPD features were not observed even at lower coverages of the adsorbate.

2.3 LEED Observations

The film ordered in one domain on the Pt(111) surface with an approximate lattice parameter of 2.8 Å, as judged from LEED patterns (Fig. 2). Due to the symmetry differences between the adsorbate the substrate, three rotated domains are expected. Their absence may be due to the substrate possessing higher index terraces biasing the grow of the film. The film thickness

was estimated to be >15 Å, as indicated by the absence of the substrate spots from the LEED pattern in the electron energy range used for data collection, 72-370 eV. LEED intensity data collection from a series of these patterns followed a standard procedure used previously with insulating thin films [7,11]. LEED data were collected at normal incidence with a crystal temperature of ≈115 K in 2 eV increments. To insure normal incidence, symmetric beams were compared to confirm that the changes in the I-V curve minima and maxima were less than or equal to 2 eV. To check that the impinging electron beam did not cause significant damage to the ordered LiF multilayer over the course of the data collection, data sets were taken while both increasing and decreasing the electron energy. It was found that peak positions deviated less than 2 eV between sets, thus providing quantitative evidence that the ordered structure remained intact during the data acquisition time period. Symmetrically equivalent beams were averaged, thus giving five symmetry inequivalent beams with a total range of 825 eV to be compared with theory. The quality of the theoretical fit to the data was quantified by the Pendry R-factor (R_P).

3. LEED THEORY

The analysis was begun by the generation of a set of phase shifts up to angular momentum l_{max}=9 for neutral Li and F using a potential derived under the muffin-tin approximation on the unreconstructed bulk LiF(100) lattice with the

Barbieri/Van Hove phase shift package. Ionic phase shifts were not considered based on previous work with iron oxides [6] which indicated that they introduced no significant changes in either the final structure or the R-factor. Inelastic scattering effects which limit the penetration depth of the incoming electrons were modeled by an imaginary part of the inner potential, here being 5 eV. Thermal effects were represented by a Debye-Waller factor (Θ_F=525 K and Θ_{Li}=450 K).

The LEED calculations were performed with the Barbieri/Van Hove symmetrized automated tensor LEED (TLEED) package [12,15]. Each layer in the (100) face of bulk-like LiF consists of a coplanar array of alternating F anions and Li cations. Each F-Li layer was defined as a composite layer. Multiple scattering within these composite layers was treated exactly through the Beeby inversion scheme. Two of these composite layers defined the interface region, where relaxations were allowed, with the lower lying composite layers constrained to their bulk positions. Scattering between pairs of composite layers was modeled with the renormalized forward scattering approximation [16].

For structural refinement, the tensor LEED approximation in combination with the Powell optimization scheme was applied. For all optimized structures, the final structure was defined as a new reference structure and the calculation was repeated, as a check on the approximation. The error bars corresponding to the vertical coordinates were calculated with Pendry's formula [17].

4. SURFACE STRUCTURAL ANALYSIS

The square symmetry of the LEED pattern along with the experimentally determined lattice constant of 2.8 Å indicated that the bulk terminated LiF(100) was the best basis for the trial structure [18]. Using the x-ray determined lattice parameter of 2.84 Å, the initial structure was constructed from ideally occupied Li and F layers. The four structural parameters that were refined were the first two intralayer corrugations (Δ_1 and Δ_2) in the first (surface) and second layer and the two topmost interlayer spacings (the spacings between the surface and the second layer and the second and third layer, $d(F_2\text{-}Li_1)$ and $d(Li_3\text{-}F_2)$, respectively). Constraining these structural parameters was the preservation of the initial structural symmetry in the resulting structures. The only nonstructural parameter that was refined was the muffin-tin zero. The phase shifts describing the scattering properties of the atoms used the electronic configuration of the neutral F and Li atoms and the muffin-tin radii equal to the atomic radii, 0.71 Å and 1.52 Å respectively [19]. Additional refinement of this model included the reduction of the muffin-tin radii of the refined layers by 10% to account for the ions' size reduction with the loss of coordination at the surface. The final structure with an R_{Pendry}=0.24, illustrated in Fig. 3 and described in Table 1, represents the structural solution of LiF(100) on Pt(111). Figure 4 compares the theoretically calculated I-V curves to the experimental curves.

The most striking difference between the surface structure and the bulk is

the buckling of the surface and second layers. The corrugation of the surface layer refined to a value of Δ_1=0.24±0.04 Å, which is 12% of the bulk interlayer spacing. This surface relaxation results from the movement of the Li atoms toward the bulk relative to the F atoms. A similar displacement of the Li atoms is responsible for the corrugation of the second layer, Δ_2=0.06±0.04 Å, by 3.0% of the bulk interlayer spacing. These modifications of the surface reduce the first interlayer spacing, d(F_2-Li_1), where the indices number the layers, from the ideal value of 2.01 Å to 1.77±0.06 Å. The second interlayer spacing, d(Li_3-F_2) is unchanged from its ideal value.

The contraction of the first interlayer spacing forces an overlap of the surface and second layer ions since the sum of the Li^+ and Cl^- ionic radii is 2.0 Å. This overlap is eliminated if there is a 10% reduction of the atomic radii in the first two layers; this degree of radii reduction is common with coordination loss in ionic solids [19]. In order to examine the amount of ion shrinkage, the surface ion size was changed indirectly by varying the muffin-tin radii of Li and F in the two topmost layers. The value of the muffin-tin radii was varied from 100% to 40% of the bulk atomic muffin-tin radii. Fig. 5 illustrates the dependence of R_P on ion shrinkage in the first two atomic layers. Very similar R_P's are found when the first two atomic layers' muffin-tin radii are allowed to be 90% and 80% of the bulk radii; R_P=0.238 and 0.239 respectively. These models share more than just similar R_P's; their interlayer and intralayer spacings are within error bars of the structure illustrated in Fig. 3. Decreasing the muffin-tin radii to below 70% of the

atomic radii yields larger R_P's with structures that have larger values for Δ_1 and smaller values for $d(F_2\text{-}Li_1)$.

For the alkali halides, the ion sizes differ greatly from their atomic counterparts. In LiF, the atomic radius of F is 0.71 Å, but the F^- radius swells to 1.4 Å; for Li, the neutral atom radius is 1.52 Å with an ionic radius of 0.6 Å. This disparity between the atomic and ionic radii was modeled indirectly in these calculations by changing the muffin-tin radii of the neutral atoms to that of the ions, but maintaining the neutral atom electronic configuration. As stated earlier, ionic charges have already been shown to have negligible effect on the structure determination of such materials[6]. After optimization, the R_P increased to a value of 0.28, and all the refined structural parameters were within error bars of the illustrated structural solution, except for the $d(F_2\text{-}Li_1)$ interlayer spacing which increased to 1.77 Å.

5. DISCUSSION

In summary, the surface structure of the multilayer LiF(100) thin film adsorbed on Pt(111) has been determined by the automated tensor LEED method. Starting with an initial trial structure consisting of an ideally terminated LiF(100) surface with the surface lattice parameter maintained at the bulk value of 2.84 Å, the refinement produced a surface with the top layer Li displaced below the F by 0.24±0.04 Å. This reconstruction is not isolated to the surface layer, but a similar

relaxation was measured in the second layer. Also in this layer , the Li is below the F, but the magnitude of the shift is reduced to 0.07±0.04 Å. These corrugations of the first and second atomic planes reduce the first interlayer spacing to 1.70±0.06 Å, a value smaller than the close-packing distance of the Li and F ions A shrinkage of the Li and F atomic radii by 10-20% allows, within error of the calculation, the accommodation of the ions in the refined distance.

The fully optimized LiF(100) structure has the same general features as that found for NaCl(100), see Table 2, [7]. Specifically, the surface corrugation results from the movement of the alkali metal ions towards the bulk. Also, there is a significant contraction of the first interlayer spacing. This contraction requires, in both LiF(100) and NaCl(100), a reduction of the ionic radii in order to accommodate the spacing.

The differences between LiF(100) and NaCl(100) are mainly seen in the magnitudes of these deviations from respective bulk structures. The corrugation of the constituent layers is not as pronounced in NaCl(100) as it is in LiF(100). The first intralayer distance in NaCl(100) is only 4.3% of an interlayer spacing compared to 12% in LiF(100). In addition, the second LiF(100) layer from the surface also exhibits a 2.5% corrugation caused by the movement of the alkali metal ions towards the bulk, a feature absent in NaCl(100). The first interlayer distance of LiF(100) is also decreased by a greater relative and absolute amount in comparison to NaCl(100). The first interlayer spacings of NaCl(100) and LiF(100) are contracted by 3.5% and 12% of the bulk interlayer spacings,

respectively. We propose that these structural differences between NaCl(100) and LiF(100) are a function of the constituent ions' polarizability. The increased polarizability of the NaCl does not require large physical shifts of the ions to compensate for the coulombic interaction loss at the surface. The more tightly bound outer shell of charge in LiF requires a movement of the ions to balance this interaction loss.

These surface layer deviations from the ideal terminations have been theoretically predicted through the application of a classical shell-and-core model of ionic systems described by Benson and Claxton [20]. Although the relative positions of the surface ions have been qualitatively predicted by this model, the actual displacements for Li and F do not agree. The theory predicted that the LiF(100) surface had a 4.8% corrugation; the measured value is 2.5 times larger. When comparing the ionic positions in the second layer, the theoretical and experimental results converge on similar values for the corrugation, 2.2% and 2.5% respectively, but the structural analysis determined that, in the second layer, the Li is below the Cl while the theory predicted the opposite (Cl^- below Li^+). Such differences between the model and real systems have been suggested by the theorists themselves, because the parameters used in the calculations were not self-consistent, thus only qualitative correlations between structure and polarizability could be concluded [20].

ACKNOWLEDGEMENT

This work was supported by the Director, Office of Science, Office of Basic Energy Sciences, Division of Materials Sciences and Engineering of the U.S. Department of Energy under contract DE-AC03-76SF00098.

REFERENCES

[1] G. E. Laramore and A. C. Switendick, *Phys. Rev. B* **7** (1973) 3615.

[2] N. Garcia, *Phys. Rev. Lett.* **37** (1976) 912.

[3] A. P. Mills, Jr. and W. S. Crane, *Phys. Rev. B* **31** (1985) 3988.

[4] S. Fölsch, U. Barjenbruch and M. Henzler, Thin Solid Films 172 (1984) 123.

[5] D. H. Fairbrother, J. G. Roberts, S. Rizzi and G. A. Somorjai, Langmuir 13 (1997) 2090.

[6] A. Barbieri, W. Weiss, M. A. Van Hove and G. A. Somorjai, Surf. Sci. 302 (1994) 259.

[7] J. G. Roberts, S. Hoffer, M. A. Van Hove and G. A. Somorjai, *Surf. Sci.* **437** (1999) 75.

[8] D. H. Fairbrother, J. G. Roberts and G. A. Somorjai, Surf. Sci. 399 (1998) 109.

[9] P. A. Redhead, *Vacuum* **12** (1962) 203.

[10] R. I. Masel, *Principles of Adsorption and Reactions on Solid Surfaces* John Wiley & Sons (1996).

[11] J. M. Powers, A. Wander, P. J. Rous, M. A. Van Hove and G. A. Somorjai, Phys. Rev. B 44 (1991) 11159.

[12] M. A. Van Hove, W. Moritz, H. Over, P. J. Rous, A. Wander, A. Barbieri, N. Materer, U. Starke, D. Jentz, J. M. Powers, G. Held and G. A. Somorjai, Surf. Sci. 287/288 (1993) 432.

[13] M. A. Van Hove, W. Moritz, H. Over, P. J. Rous, A. Wander, A. Barbieri,

N. Materer, U. Starke and G. A. Somorjai, Surf. Sci. Rep. 19 (1993) 191.

[14] P. J. Rous, M. A. Van Hove and G. A. Somorjai, Surf. Sci. 226 (1990) 15.

[15] P. J. Rous, Prog. Surf. Sci. 39 (1992) 3.

[16] M. A. Van Hove, W. H. Weinberg and C.-M. Chan, Low-Energy Electron Diffraction, Springer, Berlin, 1986.

[17] J. B. Pendry, J. Phys. C 13 (1980) 937.

[18] A. F. Ievin'sh, M. Straumanin and K. Karlson, *Zeit. fuer Physik. Chem. Abteil. B: Chem. Der Element. Aufau der Mater.* **40** (1938) 146.

[19] A. Kelly and G. W. Groves, *Crystallography and Crystal Defects*, Addison-Wesley, Reading, MA, 1970.

[20] G. C. Benson and T. A. Claxton, *J. Chem. Phys.* **8** (1968) 1356.

TABLES

Table 1. Full description of the refined LiF(100) structure. The subscripts on the atom labels correspond to the subscripts used in the text and Fig. 3.

Region[a]	Chemical Identity	Atom Number	Site Occupation	$X \pm \varepsilon_X$ (Å)[b,c]	$Y \pm \varepsilon_Y$ (Å)[b,c]	$D_Z \pm \varepsilon_Z$ (Å)[c,d]
interface	F_1	1	1	0	0	0
interface	Li_1	2	1	2.01	0	0.24±0.04
interface	F_2	3	1	2.01	0	1.70±0.06
interface	Li_2	4	1	0	0	0.07±0.04
bulk	F_3	5	1	0	0	1.93±0.06
bulk	Li_3	6	1	2.01	0	2.01
bulk	Li	7	1	0	0	2.01
bulk	F	8	1	2.01	0	0
bulk	F	9	1	0	0	2.01
bulk	Li	10	1	2.01	0	0

[a]The interface region refers to the atoms at the vacuum-solid interface that were allowed to be refined in the calculation.

[b]Absolute lateral positions of the atoms are given in two-dimensional Cartesian coordinates.

[c]The provided error bars quantify the theoretical uncertainties of the refined parameters. The absence of error bars indicates that the value was not refined in the calculation, but held constant at its bulk value

[d]The perpendicular lattice constants are defined relative to the previous atom's position, and a positive value refers to displacement towards the bulk.

Table 2. Comparison of the refined intralayer and interlayer spacings for the LiF(100) and NaCl(100) multilayer films grown on Pt(111). The labels correspond to the regions discussed in the text.

	Δ_1 (Å)[a]	Δ_2 (Å)[a]	$d(X_2\text{-}Y_1)$ (Å)[b]	$d(Y_3\text{-}X_2)$ (Å)[b]
LiF(100) on Pt(111)	0.24±0.04	0.07±0.04	1.77±0.06	1.99±0.07
NaCl(100) on Pt(111)	0.12±0.03	0.01±0.03	2.74±0.03	2.83±0.03

[a]The first and second intralayer spacings have a bulk value of 0 Å in both LiF(100) and NaCl(100)

[b]The bulk values of the interlayer spacing are 2.0 Å for LiF(100) and 2.82 Å for NaCl(100). "X" represents the compound's halogen ion, and "Y" represents the alkali metal ion.

FIGURES

Figure 1. Temperature programmed desorption profiles of a multilayer LiF film adsorbed on Pt(111).

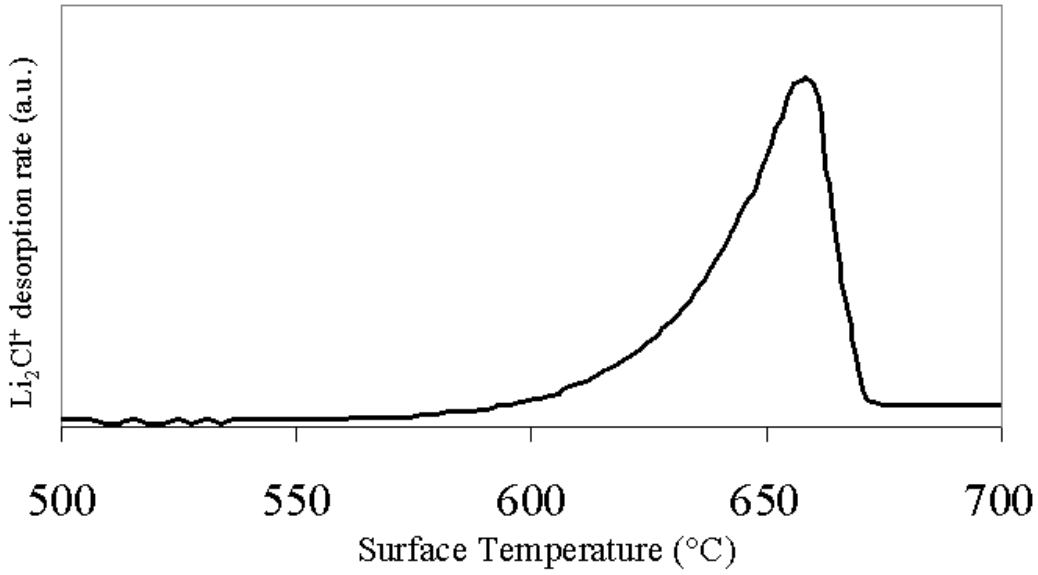

Figure 2. LEED patterns of a LiF(100) multilayer on Pt(111) recorded at an incident energy of (a) 106 eV and (b) 90 eV.

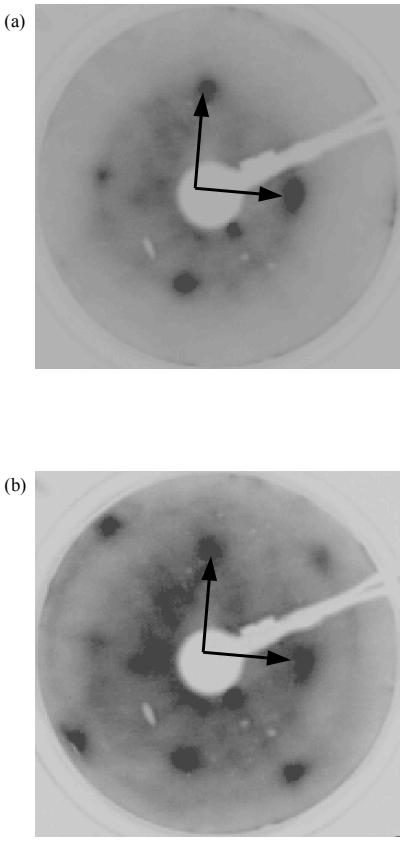

Figure 3. Side view of the optimized LiF(100) surface grown on Pt(111) (the surface termination is on top); the ionic radii were drawn full size. The values of the interlayer and intralayer spacings in the refined region are shown. The bulk spacings are $\Delta_1=\Delta_2=0.00$ Å and $d(F_2\text{-}Li_1)=d(Li_3\text{-}F_2)=2.00$ Å.

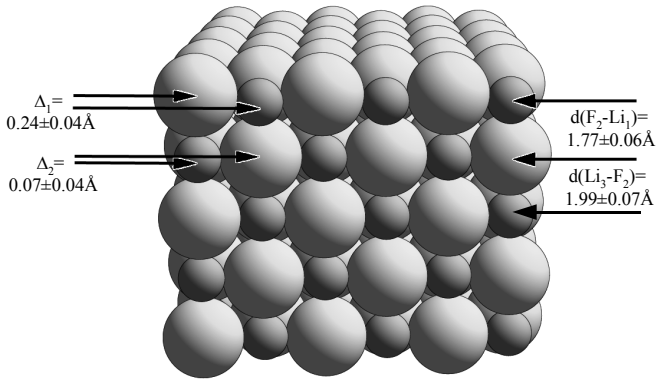

Figure 4. Comparison of the theoretical (dashed lines) and the experimental (solid lines) I-V curves of the fully optimized LiF(100) structure. All the beams used in the calculation are illustrated.

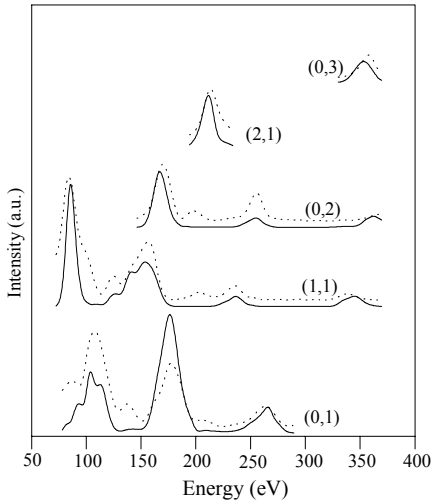

Figure 5. R-factor vs. ionic radius determining the amount of ion shrinkage in the first and second layers of LiF(100) on Pt(111).